

DECENTRALIZED CONTROLLER DESIGN FOR FORMATION FLIGHT WITH UAV FAILURE DETECTION LOGIC

Joongbo Seo, Youdan Kim, Chan Gook Park
School of Mechanical and Aerospace Engineering
Seoul National University
Seoul, 151-742 Korea

Keywords: *formation flight, graph, decentralized controller*

Abstract

This paper proposes a decentralized formation controller based on the consensus protocol and an Unmanned Aerial Vehicle(UAV) failure detection logic for formation flight. Feedback linearisation method is used to design controller to maintain a specified time-varying geometric configuration of multiple unmanned aerial vehicles. The information flow topologies between the vehicles can be defined by a Graph Laplacian matrix. An failure detection logic for formation flight is proposed, and the sudden disruption among the formation interconnections can be regulated by reforming the Graph Laplacian matrix. Stability analysis of the proposed formation controller is carried out. Numerical simulation is performed to verify the performance of the proposed controller under the dynamic formation geometry considering the failure of UAVs.

1 Introduction

Recently, there has been significant research in the area of formation flight of Unmanned Aerial Vehicles(UAVs). Formation flight is defined as a set of more than one aircraft fly whose states are coupled through a common control law. Most of the current literature on the formation flight is based on a leader-follower type controller, which is one of a centralized approaches. In this approach, one or more vehicles are designated as leaders while the others as followers[1]. In this

approach, the leader UAV tracks a predefined trajectory, and the followers track the nearest leader using the information receiving from the leader.

Although it is easy to analyze and implement the leader-follower controller, there are several advantages to decentralized approach including enhanced robustness due to the single point error from the leader's failure. The behavior-based approach, one of the decentralized scheme, was presented to achieve the formation manoeuvre for a group of mobile robots for which feedback linearisation method was considered.[2] Wei [3] studied consensus type problems for the cooperative control of mobile autonomous agents, where each agent in a team updates its information state based on those of its local neighbours. To use the information status through interconnection among the vehicles the class of directed balanced graphs is required for dealing with stability issue. Fax and Murray [4], merged the graph theory and the controller design to derive the stability criteria for formation stabilization. The interconnection between vehicles (i.e., which vehicles are sensed by other vehicles) was modeled as a graph, and the eigenvalues of the graph Laplacian matrix were analyzed to state a Nyquist-like stability criterion. Another critical problem for cooperative control is to design appropriate protocols and algorithms for each member. Verma and Wu [5] presented that the group of vehicles can converge to a consistent view of the shared information even in the presence of limited and unreliable information exchange and dynamically

changing interaction topologies.

This paper presents a decentralized controller design methodology with a failure detection logic for formation flight of UAVs. A failure detection logic for formation flight is presented in which sudden disruption among the formation interconnections can be regulated through reforming the Graph Laplacian matrix via the proposed detection logic. Also the stability analysis of the derived controller design procedures based on the Graph representation of the formation system is performed. This paper does not take into account the environmental effects such as wind gust and uncertainties from measurement noises. Numerical simulations are performed to verify the performance of the proposed formation flight controller with the UAV detection logic for the failure of interconnection among the UAVs.

An outline of this paper is as follows. Section 2 deals with the feedback linearisation of formation flight dynamics based on the nonlinear rotary wing vehicle model, and Section 3 examines the controller design procedure and the convergence analysis of the proposed consensus based controller. Section 4 describes the stability issue of the proposed controller, and Section 5 discusses how to detect the formation failure and to restructure the interconnection during the flight. Section 6 shows the simulation conditions and compares the simulation results applying the proposed detection logic with that without applying the detection logic. Concluding remarks are given in Section 7.

2 FEEDBACK LINEARISATION OF DYNAMICS

Let us consider the following a rotary-wing UAV model [2].

$$\begin{bmatrix} \dot{x}_i \\ \dot{y}_i \\ \dot{\psi}_i \\ \dot{v}_i \\ \dot{\omega}_i \end{bmatrix} = \begin{bmatrix} v_i \cos \psi_i \\ v_i \sin \psi_i \\ \omega_i \\ -\frac{v_i}{\alpha_{vi}} \\ -\frac{\omega_i}{\alpha_{\omega i}} \end{bmatrix} + \begin{bmatrix} 0 & 0 \\ 0 & 0 \\ 0 & 0 \\ \frac{1}{\alpha_{vi}} & 0 \\ 0 & \frac{1}{\alpha_{\omega i}} \end{bmatrix} \begin{bmatrix} v_i^c \\ \omega_i^c \end{bmatrix} \quad (1)$$

where a states vector is $[x_i \ y_i \ \psi_i \ v_i \ \omega_i]^T$, and a control input vector is $[v_i^c \ \omega_i^c]^T$. State variables (x_i, y_i) are the components of two-dimensional inertial position, ψ_i is a heading angle, and (v_i, ω_i) are a forward velocity and an angular velocity, respectively. Control variables v_i^c and ω_i^c are a commanded forward velocity and a commanded heading rate, respectively, and α_{vi} and $\alpha_{\omega i}$ are the position time constants that models the autopilot dynamics as the first-order time delay.

Let us derive the feedback linearisation of the nonlinear UAV model considered in this study. [2] The equations of motion in Eq.(1) can be rewritten as

$$\dot{X}_i = f(X_i) + g_i(U_i) \quad (2)$$

where $X_i = (x_i, y_i, \psi_i, v_i, \omega_i)$, and $U_i = (v_i^c, \omega_i^c)$. It is desired that the system dynamics should be nonholonomic because they do not have kinematic motion constraints and make path planning and control simpler [2]. In order to avoid the nonholonomic constraint of aerial vehicle problem introduced by Eq. (1), let us define an output variable considering the formation geometry as shown in Fig. 1. Based on the Fig. 1, the coordination of single UAV is defined as

$$r_{fi} = r_i + d_i \begin{bmatrix} \cos \psi_i \\ \sin \psi_i \end{bmatrix} \quad (3)$$

where $r_i = (x_i, y_i)$ represents *ith* UAV's CG(Center of Gravity) position in the inertial coordinates, and $r_{fi} = (x_{fi}, y_{fi})$ represents the inertial position of a point f_i having a distance d_i from the x-axis of the *ith* UAV, presuming zero pitch angle. The coordination r_{fi} is used instead of r_i to simplify the design of the formation algorithms.

After differentiation of Eq. (3) twice with respect to time, we can note that the determinant of the following matrix which coupled with input variables is not zero. And the control variables are explicitly appeared as an affine form. Therefore, the system is output feedback linearisable. [2] For feedback linearisation, let us define

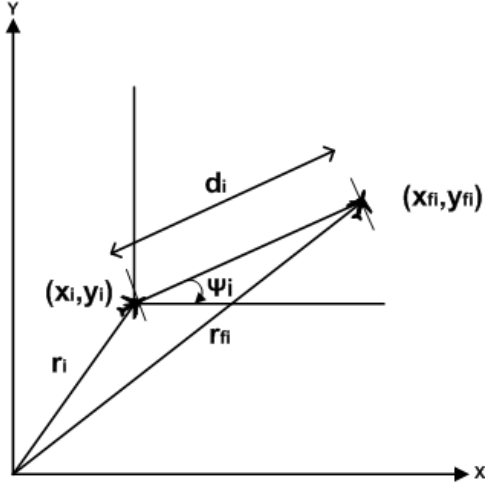


Fig. 1 Coordinate Systems for Formation Geometry

the diffeomorphic map $P: \mathbb{R}^5 \rightarrow \mathbb{R}^5$ as

$$\zeta_i = P(X_i) \triangleq \begin{bmatrix} r_{fi} \\ \dot{r}_{fi} \\ \psi_i \end{bmatrix} = \begin{bmatrix} x_i + d_i \cos \psi_i \\ y_i + d_i \sin \psi_i \\ v_i \cos \psi_i - d_i \omega_i \sin \psi_i \\ v_i \sin \psi_i + d_i \omega_i \cos \psi_i \\ \psi_i \end{bmatrix}. \quad (4)$$

The system Eq.(2) and Eq.(3) can be linearised with transformation Eq.(4). The output feedback linearizing control can be given by

$$u_i = g_i^{-1}(\mu_i - f) \quad (5)$$

$$u_i \triangleq \begin{bmatrix} v_i^c \\ \omega_i^c \end{bmatrix} = \begin{bmatrix} \frac{\cos \psi_i}{\alpha_{vi}} & -\frac{d_i \sin \psi_i}{\alpha_{\omega_i}} \\ \frac{\sin \psi_i}{\alpha_{vi}} & \frac{d_i \cos \psi_i}{\alpha_{\omega_i}} \end{bmatrix}^{-1} \begin{bmatrix} \mu_i - \\ \left(-\frac{v_i}{\alpha_{vi}} \cos \psi_i + \frac{d_i}{\alpha_{\omega_i}} \omega_i \sin \psi_i - v_i \omega_i \sin \psi_i - d_i \cos \psi_i \omega_i^2 \right) \\ \left(-\frac{v_i}{\alpha_{vi}} \sin \psi_i - \frac{d_i}{\alpha_{\omega_i}} \omega_i \cos \psi_i + v_i \omega_i \cos \psi_i - d_i \sin \psi_i \omega_i^2 \right) \end{bmatrix} \quad (6)$$

where μ_i is an additional control input which can be designed for formation flight.

Using Eq. (4) and Eq. (6) gives

$$\begin{bmatrix} \dot{\zeta}_{1i} \\ \dot{\zeta}_{2i} \end{bmatrix} = \begin{bmatrix} \zeta_{3i} \\ \zeta_{4i} \end{bmatrix} \quad (7)$$

$$\begin{bmatrix} \dot{\zeta}_{3i} \\ \dot{\zeta}_{4i} \end{bmatrix} = \mu_i \quad (8)$$

$$\dot{\zeta}_{5i} = -\frac{1}{d_i} \zeta_{3i} \sin \zeta_{5i} + \frac{1}{d_i} \zeta_{4i} \cos \zeta_{5i} \quad (9)$$

Equation (9) represents the internal dynamics which are rendered unobservable and uncontrollable by the transformation Eq. (4). The zero dynamics are found by setting $\zeta_{1i} = \zeta_{2i} = \zeta_{3i} = \zeta_{4i} = 0$, then $\dot{\zeta}_{5i} = 0$. Therefore, zero dynamics are stable but not asymptotically stable. Note from $\zeta_{5i} = \psi_i$ and $(\zeta_{3i}, \zeta_{4i})^T$ represents the velocity, this implies that the angle ψ_i will not change when the position of UAV stops moving. The control law will be designed in Section 3 such that a team of several UAVs can fly with a pre-defined formation velocity given by $v_f^d(t)$, and the team can preserve a time-varying geometric configuration during the flight.

3 CONTROL LAW DESIGN FOR CONSENSUS FORMATION FLIGHT

3.1 Graph Theory

In this research, a graph representation is used to express the connection between the formation agents and to compute the stability issue.

To get the Laplacian matrix, an adjacency matrix should be computed for a simple graph. Directed graph $G = (V, E)$ consists of a finite, nonempty set of *vertices* V and a set of *edges* E . Each edge is an ordered pair (v, w) of vertices. The adjacency matrix of graph G , whose vertices are explicitly ordered v_1, v_2, \dots, v_n , is the $n \times n$ matrix A_G such that

$$A_G(i, j) = \begin{cases} 1 & \text{if } v_i \text{ and } v_j \text{ are adjacent} \\ 0 & \text{otherwise} \end{cases}$$

where a vertex v_i is *adjacent* to vertex v_j if they are joined by an edge. The Laplacian matrix L is a square matrix whose rows and columns correspond to the vertices of a graph. A diagonal entry is the degree of the corresponding vertex; an off-diagonal entry is -1 if the corresponding vertices are adjacent and 0 otherwise. In other words, $L = D - A$, where D is the diagonal matrix of degrees of the vertices and A is the usual adjacency matrix.[6] Graph Laplacian matrix L is a positive definite matrix as

$$L \triangleq [l_{ij}], \quad l_{ii} = k \quad \text{and} \quad l_{ij} = -g_{ijk}, \quad \forall i \neq j \quad (10)$$

where $k > 0$, $g_{ii} \triangleq 0$, $g_{ij} = 1$ if the information flows from vehicle j to vehicle i , and $g_{ij} = 0$ otherwise, $\forall i \neq j$.

3.2 Control Law Design with Consensus Protocol

Let us consider the dynamics of each vehicle,

$$\begin{aligned}\dot{r}_i &= v_i \\ \dot{v}_i &= u_i\end{aligned}\quad (11)$$

where $r_i \in \mathbb{R}^m$ and $v_i \in \mathbb{R}^m$ denote the position and velocity of i -th vehicle, respectively.

$$r_i = r_{oi} + r_{iF} \quad (12)$$

where r_{oi} denotes the position of formation center, and r_{iF} denotes a vector from the formation center to the i -th node. Consensus is achieved when r_{oi} of each vehicle has the same position r_o . Let us consider the following control input of the i th vehicle.

$$\begin{aligned}u_i &= \ddot{r}_{iF} + \dot{v}_{iF} - \alpha(\dot{r}_i - \dot{r}_{iF} - v_{iF}^d) - \beta(r_i - r_{iF} - \int v_{iF}^d dt) \\ &\quad - \sum_{j=1}^n g_{ijk} \{ [(r_i - r_{iF}) - (r_j - r_{jF})] + \gamma[(v_i - \dot{r}_{iF}) - (v_j - \dot{r}_{jF})] \}\end{aligned}\quad (13)$$

where $v_{iF}^d \in \mathbb{R}^m$ is a nominal formation velocity, α, β, γ are positive constant gains, and g_{ij}, k are determined by the Laplacian graph. Substituting Eq. (13) in Eq. (11), we have

$$\begin{aligned}(\ddot{r}_{oi} - \ddot{v}_{iF}^d) + \alpha(\dot{r}_{oi} - \dot{v}_{iF}^d) + \beta(r_{oi} - \int v_{iF}^d dt) \\ + \sum_{j=1}^n g_{ijk} \{ [(r_i - r_{iF}) - (r_j - r_{jF})] \\ + \gamma[(v_i - \dot{r}_{iF}) - (v_j - \dot{r}_{jF})] \} = 0.\end{aligned}\quad (14)$$

The first three terms of Eq. (14) makes errors zero between each vehicle's formation center and velocity, and acceleration. The remaining summation part can be considered as an external disturbance which guarantees the minimum consensus error with the neighbourhood vehicles.

3.3 Convergence Analysis of Control Law with Consensus Protocol

Let us analyze the convergence of the proposed control law. Equations (11)-(13) can be rewritten as a double integrator. For simplicity, let us introduce the following variables

$$z_i = r_i - \int v_{iF}^d dt \quad (15)$$

Differentiating Eq. (15) twice with respect to time yields

$$\ddot{z}_i = \ddot{r}_i - \ddot{v}_{iF}^d \quad (16)$$

Using Eq. (13) in Eq. (16), the final closed-loop dynamics can be obtained as follows.

$$\begin{aligned}(\ddot{z}_i - \ddot{r}_{iF}) + \alpha(\dot{z}_i - \dot{r}_{iF}) + \beta(z_i - r_{iF}) \\ + \sum_{j=1}^n g_{ijk} \{ [\xi_i - r_{iF}] - [\xi_j - r_{jF}] \\ + \gamma[(\dot{\xi}_i - \dot{r}_{iF}) - (\dot{\xi}_j - \dot{r}_{jF})] \} = 0\end{aligned}\quad (17)$$

Now, let us introduce an error variable as

$$e_i \triangleq z_i - r_{iF}. \quad (18)$$

Substituting Eq. (18) into Eq. (17) gives

$$\ddot{e}_i + \alpha\dot{e}_i + \beta e_i + \sum_{j=1}^n g_{ijk} \{ (e_i - e_j) + \gamma(\dot{e}_i - \dot{e}_j) \} = 0. \quad (19)$$

The goal of the consensus protocol is to guarantee that $e_i \rightarrow 0$, $e_j \rightarrow 0$ as $t \rightarrow \infty$, which is equivalent to $z_i - r_{iF} \rightarrow 0$ and $\dot{z}_i - \dot{r}_{iF} \rightarrow 0$ as $t \rightarrow \infty$, or, $r_{oi} - \int v_{iF}^d dt \rightarrow 0$ and $\dot{r}_{oi} - v_{iF}^d \rightarrow 0$. Then, we have $r_{oi} \rightarrow r_{oj}$, $\dot{r}_{oi} \rightarrow \dot{r}_{oj}$. in order to achieve the aforementioned property of the closed-loop dynamics. In the subsequent section, the criteria of the control gains α, β and γ will be discussed.

4 STABILITY CRITERIA OF FORMATION CONTROL GAINS

Let us analyze the stability criteria of the proposed formation flight controller. Equation (19) can be rewritten as

$$\frac{d}{dt} E \triangleq \Gamma E \quad (20)$$

where $E \triangleq [e_1 \ e_2 \ \cdots \ e_n \ e_1 \ e_2 \ \cdots \ e_n]^T$ and

$$\Gamma = \begin{bmatrix} 0_{n \times n} & I_n \\ -\alpha I_n - L & -\beta I_n - \gamma L \end{bmatrix}. \quad (21)$$

The gain parameters, α , β , γ , and the graph Laplacian matrix L should be properly chosen such that all eigenvalues of Γ placed on the left half plane. Note that α , β , γ are positive real constants. The several information exchange topologies between the UAVs can be considered as shown in Fig. 2.

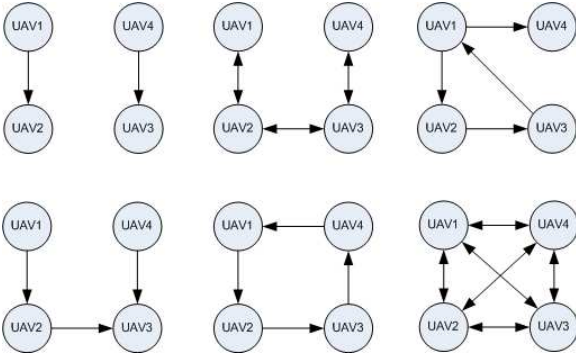


Fig. 2 Various Information Types Between Four UAVs Case

Taking into account the measurements from sensors with the limited field of views or random communication losses, an unidirectional information flow topology is considered in this study. Graph Laplacian matrix L can be determined by the method explained in the preceding section 3.1. Once, the information of its own and at least one of another vehicle are available from L , it is possible to set the value of α , β , and γ . The eigenvalues of L can be computed using the following equation

$$\begin{aligned} \det(sI_{2n} - \Gamma) &= \det \left(\begin{bmatrix} sI_n & -I_n \\ \alpha I_n + L & sI_n + \beta I_n + \gamma L \end{bmatrix} \right) \\ &= \det((s^2 + s\beta + \alpha)I_n + (s\gamma + 1)L) = 0 \end{aligned} \quad (22)$$

Note that

$$\det(sI_n + L) = \prod_{i=1}^n (s - \lambda_i) \quad (23)$$

where λ is the eigenvalue of $-L$. By comparing Eq. (22) with Eq. (23), we have

$$\begin{aligned} &\det\{((s^2 + s\beta + \alpha)I_n + (s\gamma + 1)L)\} \\ &= \prod_{i=1}^n [(s^2 + \beta s + \alpha) - (s\gamma + 1)\lambda_i] \end{aligned} \quad (24)$$

Then, the roots of Eq. (22) can be obtained as

$$s_{i\pm} = \frac{(\gamma\lambda_i - \beta) \pm \sqrt{(\gamma\lambda_i - \beta)^2 - 4(\alpha - \lambda_i)}}{2} \quad (25)$$

For the matrix Γ to be positive definite, the parameters α , β , and γ should satisfy the following relations.

- Case I) $(\gamma\lambda_i - \beta)^2 - 4(\alpha - \lambda_i) > 0$
 $(\gamma\lambda_i - \beta) \pm \sqrt{(\gamma\lambda_i - \beta)^2 - 4(\alpha - \lambda_i)} < 0$
- Case II) $(\gamma\lambda_i - \beta)^2 - 4(\alpha - \lambda_i) \leq 0$
 $\gamma\lambda_i - \beta < 0 \quad i = 1 \dots n$

Using the guidelines of Case I), Case II), and Eq. (25), the control gain (α , β , γ) can be decided.

5 DETECTION LOGIC AND INTERCONNECTION RESTRUCTURING FOR UAV FAILURE

According to the Fault Detection and Isolation(FDI) theory, fault detection refers to the decision of whether a fault occurs or not. And fault isolation is the process of finding and excluding the failed component. Note that this study considers the case in which one of vehicles totally broke down. Once the failure is detected, the failed vehicle should be isolated. It means the information of the failed vehicle is no longer available after the isolation. In the rotary wing vehicle model considered in this study, the range of velocity is in the low ($= \pm 5m/s$) level. Hence, it needs a proper time duration to make an error level sensible. A time duration variable T_{buffer} as

a buffer concept is useful to determine the status of each vehicle. In this study, the time duration is set as $T_{buffer} = 5sec$ for which the comparison process is performed. Then the detection logic with the present connectivity starts to operate directly. Since the computation time for the control gain design is quite shorter than T_{buffer} , the controller can still produce the appropriate response without performance degradation.

Figure 3 shows the possible time-varying interconnection and formation geometry between each UAV, which resulted from the failure of UAV1 and UAV5.

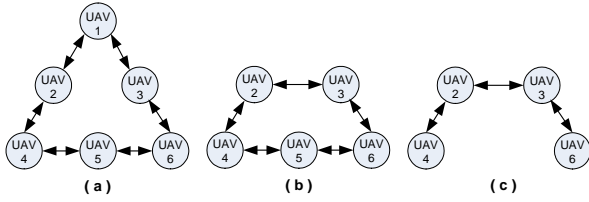


Fig. 3 Information Exchange Scenario

Equation (26) remarks on the Index value generation of Figure 3(a) to determine if each of UAV collapses or not.

$$\left\{ \begin{array}{l} \{Index1 | 1, 2, 3\} \\ \{Index2 | 1, 2, 4\} \\ \{Index3 | 1, 3, 6\} \\ \{Index4 | 2, 4, 5\} \\ \{Index5 | 4, 5, 6\} \\ \{Index6 | 3, 5, 6\} \end{array} \right\} \triangleq \left\{ \begin{array}{l} |(d_{12} + d_{23} + d_{31}) - D_1| \\ |(d_{12} + d_{24} + d_{41}) - D_2| \\ |(d_{13} + d_{36} + d_{61}) - D_3| \\ |(d_{24} + d_{45} + d_{52}) - D_4| \\ |(d_{45} + d_{56} + d_{64}) - D_5| \\ |(d_{35} + d_{56} + d_{63}) - D_6| \end{array} \right\} \quad (26)$$

where $d_{ij} = \|\bar{x}_i - \bar{x}_j\|$, \bar{x}_i is a position vector of vehicle i , and D_i means the summation of the desired relative distance among the vehicle i and its relevant neighbour. Note that each index consists of an orthogonal combination of UAVs. In the definition of Eq. (26), each index value comprises of an independent combination of UAV information which can assure faithful detection theoretically. To find out whether each vehicle breaks away, each index value is compared with a proper adaptive threshold value T_i as

$$\frac{Index\ i}{N} \geq T_i(\psi, V) \quad (27)$$

where N is the number of UAVs involved in the index. Threshold value T_i is considered as the

function of heading angle and velocity. Equation (28) is considered to decide whether each UAV is failed or not.

$$T_i(\psi) = \frac{T_{max}^{\psi} - T_{min}^{\psi}}{\psi_{max} - \psi_{min}} (\psi - \psi_{min}) + T_{min}^{\psi} \quad (28)$$

where T_{max}^{ψ} is selected when ψ is maximum, T_{min}^{ψ} for when ψ has minimum value. Especially, Eq. (29) is the specific case of (28), for the wingman agent in formation geometry. T_{max}^{ψ} , T_{min}^{ψ} , T_{max}^V and T_{min}^V can be collected from the coordinated turn flight simulations without any failure of vehicles.

$$T_i(V) = \frac{T_{max}^V - T_{min}^V}{V_{max} - V_{min}} (V - V_{min}) + T_{min}^V \quad (29)$$

where T_{max}^V can be selected when V is maximum, T_{min}^V for when V has minimum value.

Equations(28) and (29) use the maximum and minimum value of it to prevent the false alarm when the vehicle manoeuvres in a vertical way like hovering or has a tiny distance error. In this study, we considered the simulation scenario which has two UAV failures during the whole flight, and therefore the threshold value should be re-computed using the varying interconnection topology as shown in Fig. 3. Equation (30) remarks on the index value generation for the case of Figure 3(b).

$$\left\{ \begin{array}{l} \{Index2 | 2, 3, 4\} \\ \{Index3 | 2, 3, 6\} \\ \{Index4 | 2, 4, 5\} \\ \{Index5 | 4, 5, 6\} \\ \{Index6 | 3, 5, 6\} \end{array} \right\} \triangleq \left\{ \begin{array}{l} |(d_{23} + d_{24} + d_{43}) - D_2| \\ |(d_{23} + d_{36} + d_{62}) - D_3| \\ |(d_{24} + d_{45} + d_{52}) - D_4| \\ |(d_{45} + d_{56} + d_{64}) - D_5| \\ |(d_{36} + d_{56} + d_{53}) - D_6| \end{array} \right\} \quad (30)$$

And, Eq. (31) is for the case of Fig. 3(c).

$$\left\{ \begin{array}{l} \{Index2 | 2, 3, 4\} \\ \{Index3 | 2, 3, 6\} \\ \{Index4 | 2, 4\} \\ \{Index6 | 3, 6\} \end{array} \right\} \triangleq \left\{ \begin{array}{l} |(d_{23} + d_{24} + d_{43}) - D_2| \\ |(d_{23} + d_{36} + d_{62}) - D_3| \\ |(d_{24}) - D_4| \\ |(d_{36}) - D_6| \end{array} \right\} \quad (31)$$

Now, let us inspect how to decide a new interconnection between the formation members when the disconnected event happens. During the flight, several failures may happen consecutively. In this case, it is required to set up the guideline

of how, the vehicle which loses information exchange line, can get the new connection. The priority should be given to a proper agent to achieve the stable connectivity. Figure 4 shows the reconnection priority when UAVs are in failure.

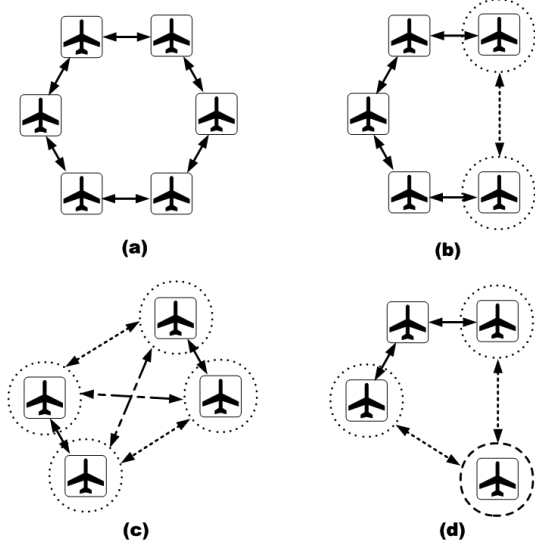


Fig. 4 How to Decide the Next Interconnection

In Figure 4, the vehicles losing the connection are marked with dotted circle. Figure 4(a) is the interconnection topology without the failure. Figure 4(b) shows the method restructuring the topology in the case of one disconnection in the formation. Figures 4(c) and 4(d) show the case of two disconnections. To find a new connection, the criterion are considered like as follows.

It is admissible assumption to set the finite range of detection for each agent. During the flight, each vehicle can monitor the information data from the available neighbourhood vehicles within the range of detection. Let us assume that the each vehicle i can get the signal from K_i vehicles where K_{def} is the default number of signals at the start of the flight.

I . Find K_i which

$$\min K_i < K_{def}, \quad \{i = 1 \dots N\} \quad (32)$$

then renew the connection with vehicle i .

II . If multiple $\{K_i : \|\min K_i < K_{def}\}$ exist, then renew the connection with the vehicle which locates closer.

where N is the number of vehicle which can be detected in the range of detection. Figure 4 shows the restructuring of interconnection according to the rule of Eq. (32).

6 NUMERICAL SIMULATION RESULT

6.1 Simulation conditions

The parameter values used in the simulation are summarized in Table 1. This simulation considers two failures of the formation members : UAV 1 at $T = 85sec$, and UAV 5 at $T = 135sec$. Also, three turn motions are performed at $T = 50sec$, $T = 110sec$ and $T = 170sec$. The UAVs are arranged initially in a big triangle. The formation geometry is chosen as

$$\theta_1(t) = \begin{cases} 0 & t \leq 50 \text{ sec} \\ \frac{t-50}{\frac{15}{\pi}} & 50 < t < 50 + \frac{15\pi}{2} \text{ sec} \\ \frac{15\pi}{2} & t > 50 + \frac{15\pi}{2} \text{ sec} \end{cases}$$

$$\theta_2(t) = \begin{cases} 0 & t \leq 110 \text{ sec} \\ \frac{t-110}{\frac{15}{\pi}} & 110 < t < 110 + \frac{15\pi}{2} \text{ sec} \\ \frac{15\pi}{2} & t > 110 + \frac{15\pi}{2} \text{ sec} \end{cases}$$

$$\theta_3(t) = \begin{cases} 0 & t \leq 170 \text{ sec} \\ \frac{t-170}{\frac{15}{\pi}} & 170 < t < 170 + \frac{15\pi}{2} \text{ sec} \\ \frac{15\pi}{2} & t > 170 + \frac{15\pi}{2} \text{ sec} \end{cases}$$

$$R_i(\theta_i(t)) = \begin{bmatrix} \cos(\theta_i(t)) & \sin(\theta_i(t)) \\ -\sin(\theta_i(t)) & \cos(\theta_i(t)) \end{bmatrix}$$

Parameter	Value
v_i^c	$v_i^c \in [-5, 5] m/s$
r_i^c	$r_i^c \in [-1, 1] rad/s$
v_F^d	$2 * [\sin(\theta_1(t)), \cos(\theta_1(t))]$
r_{1F}	$R_3 R_2 R_1 [0, 7\sqrt{3}]^T$
r_{2F}	$R_3 R_2 R_1 [-7, 0]^T$
r_{3F}	$R_3 R_2 R_1 [7, 0]^T$
r_{4F}	$R_3 R_2 R_1 [-14, -7\sqrt{3}]^T$
r_{5F}	$R_3 R_2 R_1 [0, -7\sqrt{3}]^T$
r_{6F}	$R_3 R_2 R_1 [14, -7\sqrt{3}]^T$

Table 1 Parameter values used in simulation

6.2 Comparison with Detection-free case

By recognizing the failure event of UAVs, a new formation geometry and the corresponding Laplacian matrix are constructed in real time. Accordingly, the control gains can be decided with criterion shown in Sec. 5. Figure 5 shows that the formation is preserved with the desired time-varying geometry including the UAV failure detection logic, and each UAV flies with a nominal formation velocity. Note that UAV4 and UAV6 try to move for keeping the relative velocity to the others at the turning corners. After detection of the communication failures of UAV1, UAV2 and UAV3 begin to have a new network to maintain a formation.

On the contrary to Fig.5, each UAV could not keep the relative velocity and distance without the detection logic as shown in Figure6. Figure 7 shows the values of distance between six vehicles without the failure detection logic. The distance unrelated with the failed vehicles, UAV1 and UAV5, showed the poor performance after the failures. From Fig. 10 and 11, it can be seen that the heading angle response of the detection-free case is unstable and oscillatory compared to the case with the detection logic. Figure 8 shows the result of failure detection history. Right after T_{buffer} seconds from the disconnected moment, the failure decision is carried out immediately. Table 2 shows the values of T_{min} and T_{max} using in the simulation. As stated in Eqs. (28) and (29) the threshold values of each UAV are determined. Figure 9 shows index and threshold value histories for each vehicle. Note that the momentary peak responses of the index value could be resulted from the turning movements.

	Param.	Value	Param.	Value
UAV1	T_{min}^{θ}	0	T_{max}^{θ}	2.1236
UAV2	T_{min}^{θ}	0	T_{max}^{θ}	33.3846
UAV3	T_{min}^{θ}	0	T_{max}^{θ}	12.4137
UAV4	T_{min}^V	0	T_{max}^V	20.3799
UAV5	T_{min}^{θ}	0	T_{max}^{θ}	22.5937
UAV6	T_{min}^V	0	T_{max}^V	4.0861

Table 2 T_{min} and T_{max} values used to make Threshold values for each UAV

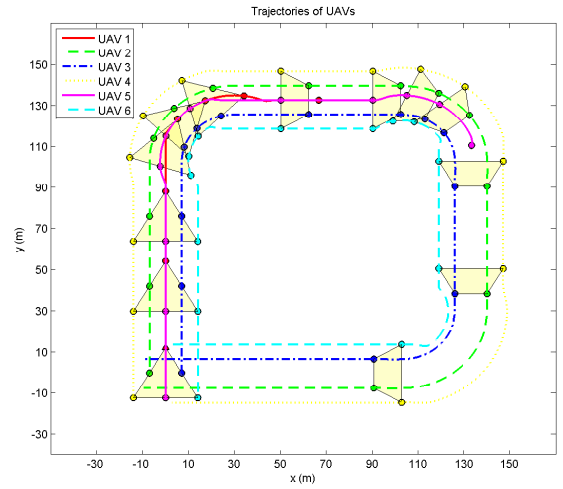


Fig. 5 Trajectories of Each UAV With Detection Logic

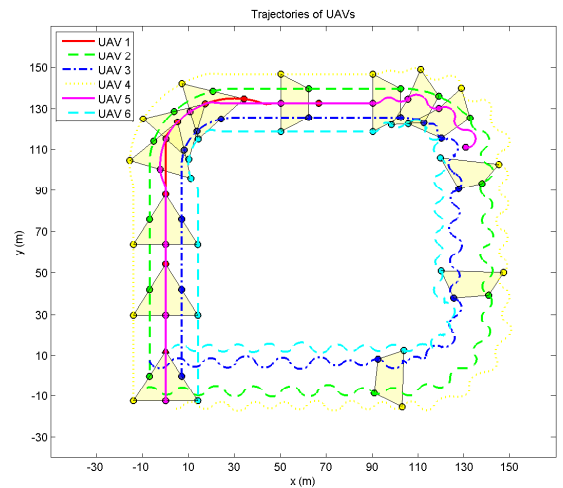


Fig. 6 Trajectories of Each UAV Without Detection Logic

Decentralized Controller Design for Formation Flight with UAV Failure Detection Logic

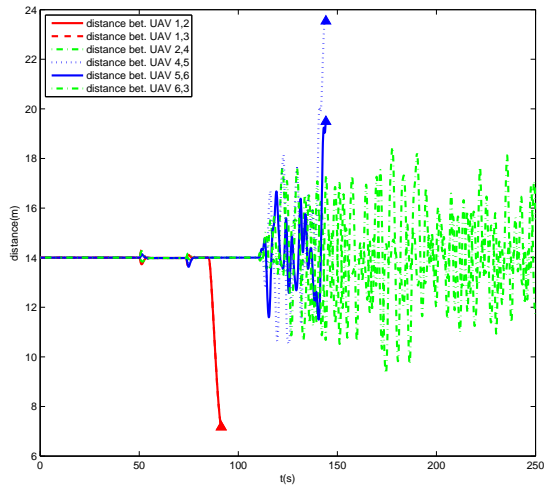


Fig. 7 Distance Between UAVs Without Detection Logic

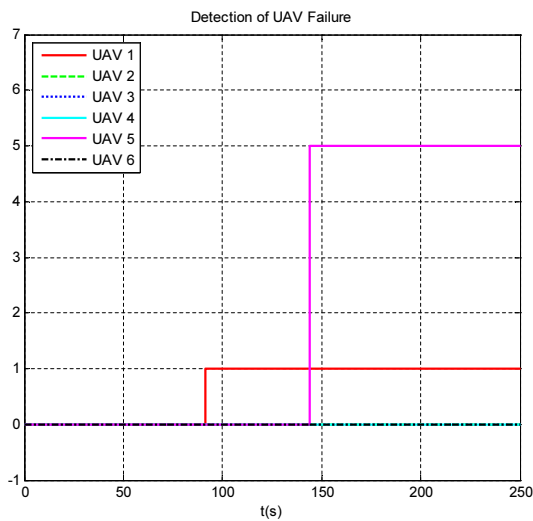


Fig. 8 Failure Detection Profiles of UAVS

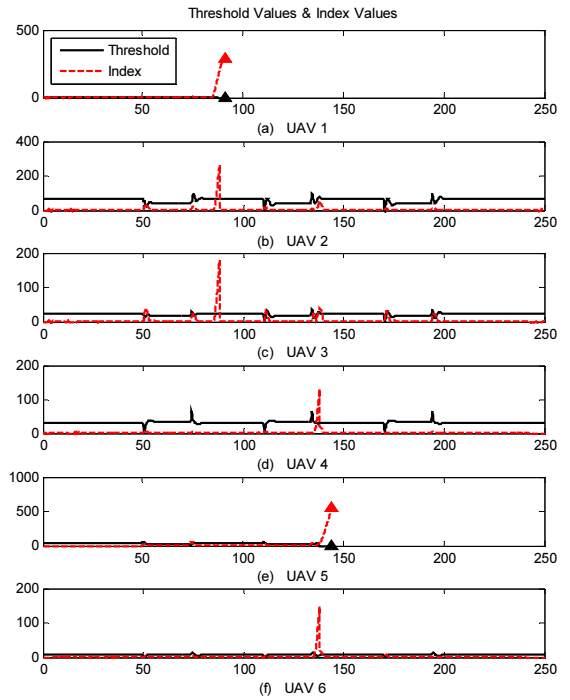


Fig. 9 Comparison of Threshold and Index Values of UAV 1-6

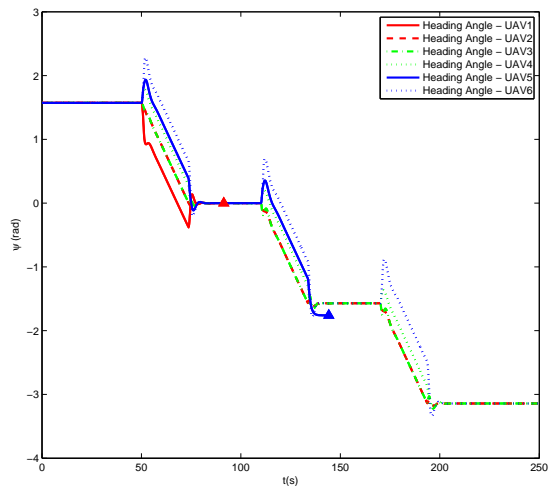


Fig. 10 Heading Angle Histories of Each UAV With Detection Logic

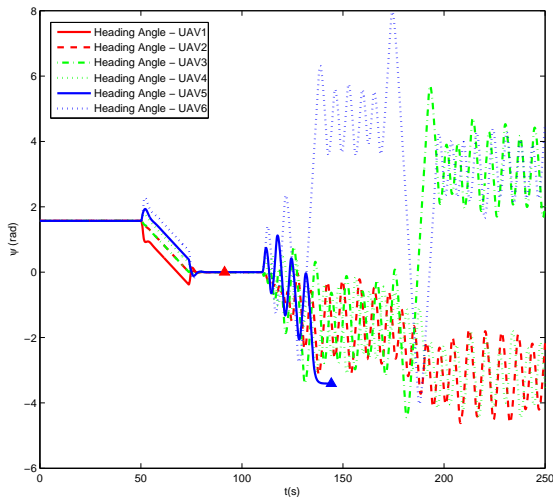


Fig. 11 Heading Angle Histories of Each UAV Without Detection Logic

7 CONCLUSION

The decentralized formation flight controller is designed for the formation of the unmanned aerial vehicles. The failure detection logic is proposed considering the change of interconnection topology between neighbourhood vehicles in the formation fleet. In order to maintain stable formation, the guidelines for controller design is proposed via the graph representation. This approach is useful in dealing with sudden break downs or disconnections between the members during the formation flight, and it could be applicable to the ground robotics, satellites and missiles as well as UAVs. To apply the proposed technique to the real-field applications, the external disturbance such as wind effects, the measurement noises and communication time delay are to be considered with the UAV failure detection. Besides, a three-dimensional model will be studied to detect the vertical failures with three-dimensional states and an extra degree of freedom as further works.

8 Acknowledgement

This work was supported by the Defense Research Grant funded by the Agency for Defense

Development, Korea.

9 Copyright Statement

The authors confirm that they, and/or their company or organization, hold copyright on all of the original material included in this paper. The authors also confirm that they have obtained permission, from the copyright holder of any third party material included in this paper, to publish it as part of their paper. The authors confirm that they give permission, or have obtained permission from the copyright holder of this paper, for the publication and distribution of this paper as part of the ICAS2010 proceedings or as individual off-prints from the proceedings.

References

- [1] Wang, P. K. C. and Hadaegh, F. Y. Coordination and control of multiple micro-spacecraft moving in formation, *The Journal of the Astronautical Sciences*, Vol. 44, No. 3, 1996, pp. 315-355.
- [2] Lawton, J. R., Beard, R. W. and Young, B. A decentralized approach to formation maneuvers, *IEEE Transactions on Robotics and Automation*, Vol. 19, No. 6, 2003, pp. 933-941.
- [3] Ren, W. and Atkins, E. Second-order consensus protocols in multiple vehicle systems with local interactions, AIAA Guidance, Navigation, and Control Conference, San Francisco, CA, August 2005.
- [4] Fax, J. A. and Murray, R. M. Graph Laplacians and stabilization of vehicle formations, IFAC World Congress, Barcelona, Spain, June 2002.
- [5] Verma, A. and Wu, C. Autonomous command and control system for UAV formation, AIAA Atmospheric Flight Mechanics Conference, Austin, TX, August 2003.
- [6] Gross, J.L. and Yellen, J. *Handbook of graph theory*, CRC Press, Boca Raton, FL, 2004.